# Modeling and experimental verification of an ultra-wide bandgap in 3D phononic crystal

L. D'Alessandro, E. Belloni, R. Ardito, A. Corigliano, and F. Braghin

# Modeling and experimental verification of an ultra-wide bandgap in 3D phononic crystal

L. D'Alessandro,[1] E. Belloni,[2,a)] R. Ardito,[1] A. Corigliano,[1] and F. Braghin[2]

[1]Department of Civil and Environmental Engineering, Politecnico di Milano, Milano 20133, Italy
[2]Department of Mechanical Engineering, Politecnico di Milano, Milano 20156, Italy

This paper reports a comprehensive modeling and experimental characterization of a three-dimensional phononic crystal composed of a single material, endowed with an ultra-wide complete bandgap. The phononic band structure shows a gap-mid gap ratio of 132% that is by far the greatest full 3D bandgap in literature for any kind of phononic crystals. A prototype of the finite crystal structure has been manufactured in polyamide by means of additive manufacturing technology and tested to assess the transmission spectrum of the crystal. The transmission spectrum has been numerically calculated taking into account a frequency-dependent elastic modulus and a Rayleigh model for damping. The measured and numerical transmission spectra are in good agreement and present up to 75 dB of attenuation for a three-layer crystal. *Published by AIP Publishing.*
[http://dx.doi.org/10.1063/1.4971290]

The study of wave propagation along the spatially periodic structures[1] is of great interest for solid state physics while approaching the influence of atomic vibration on crystal properties.[2] The peculiar property of these structures is the formation of bandgaps, i.e., portions of the frequency response for which an incident wave cannot propagate through the crystal. This idea is used in several applications in the electromagnetic domain, namely, the so-called photonic crystals (PtCs), to build waveguides, mirrors, and filters.[3] More recently,[4,5] large interest has been devoted to phononic crystals[6] (PnCs). Formally, a phonon is a quasi-particle that describes the vibrational state of a lattice. Therefore depending on dimensions and materials of the crystal structure, applications range from vibrations suppression to noise isolation, from acoustic diodes to thermal meta-materials.[7] A third class, the so-called phoxonic crystals (PxCs), is nowadays becoming popular due to the interaction between phonons and photons.[8–11]

It is undeniable that bandgap width is a key factor to boost performances and robustness, i.e., wider bandgap means stronger attenuation around the gap central frequency.[12–14] Width of a bandgap can be expressed using the gap-mid gap ratio, a non-dimensional parameter that avoids frequency dependence

$$BG\% = \frac{2(f_{top} - f_{bot})}{f_{top} + f_{bot}}\%, \qquad (1)$$

where $f_{top}$ and $f_{bot}$ are the bounding frequencies of the bandgap. A 3D crystal with a full bandgap guarantees wave scattering in all directions,[3,6,15] as it is demonstrated in several 3D structures for the photonic applications. To broaden the bandgap size in phononic crystals, acoustic or elastic impedance mismatch between portions of the structure is essential: an array of steel spheres in an epoxy matrix shows a bandgap with a ratio of 66.7%,[6] while a similar system

with steel spheres in plastic matrix presents a ratio between 33.0% and 50.2% depending on the geometry and material choice.[16] Polyimide, polyamide, and bronze tube structure shows a bandgap with ratio equal to 54.5%.[17] In order to use a single material, the crystal geometry must be optimized using suitable ratios between regions of material and voids. A cube with cylindrical holes shows a complete phononic bandgap with a ratio around 27.3% in simulation and somewhat wider in experiments.[18] A gap-mid gap ratio of about 50.4% is achieved by a silicon rubber phononic crystal.[19] As a last example, a simple cubic lattice with optimized geometrical parameters numerically shows a full bandgap with gap-mid gap ratio of 82.1% for phononic and 11.4% for photonic.[20] These results are summarized in Table I.

The topology presented in this work is the three-dimensional generalization of an optimal shape, in terms of gap-mid gap ratio, for in-plane periodic single material elastic phononic crystals.[21] The fundamental unit cell topology could be approximated by means of an external frame with half circles centered in the middle-point of the edges (see Fig. 1(a)). The optimization process sets the following internal proportions: the frame thickness as $t = 0.05\,a$, the radius of the circle as $s = 0.33\,a$, where $a$ is the unit cell characteristic dimension.[22] In order to build a three-dimensional phononic

TABLE I. Examples of bandgaps in photonic, phononic, and phoxonic crystals.

| References | Type | Gap-mid gap ratio |
|---|---|---|
| Laude[6] | PnC[a] | 66.7% |
| Zhang et al.[16] | PnC | 33.0–50.2% |
| Delpero et al.[17] | PnC | 54.5% |
| Lucklum and Vellekoop[18] | PnC | 27.3% |
| Babaee et al.[19] | PnC | 50.4% |
| Ma et al.[20] | PxC[b] | 82.1% PnC and 11.4% PtC[c] |

[a]Phononic crystal.
[b]Phoxonic crystal.
[c]Photonic crystal.

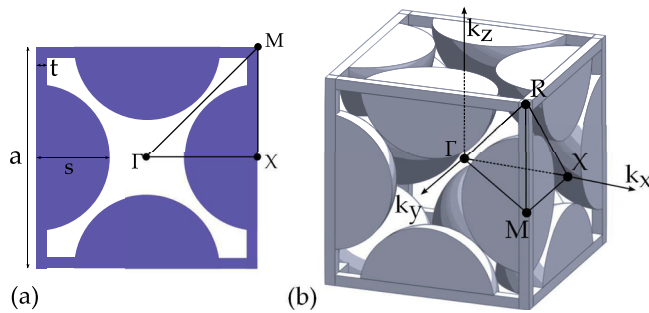a)Electronic mail: edoardo.belloni@polimi.it

FIG. 1. (a) Optimized unit cell topology for in-plane periodic single material phononic crystal. (b) Unit cell topology for the three-dimensional periodic phononic crystal. The Irreducible Brillouin Zones for both the cases are highlighted.

crystal, the symmetries and proportions are maintained ending up with a cubic structure where each face is the planar topology of Fig. 1(a) properly extended, i.e., the half circles are extended to quarters of spheres (see Fig. 1(b)). The non-dimensional phononic band structure of the crystal with a unit cell of Fig. 1(b) is reported in Fig. 2. It is calculated by means of a finite element (FE) analysis repeating the simulation both with the Solid Mechanics Module of COMSOL Multiphysics v5.2 and ANSYS Mechanical APDL v16 in order to double-check the results. In COMSOL, the phononic band structure can be obtained by imposing Floquet periodic boundary conditions and performing a parametric sweep over the wave vector, while in ANSYS, a proper macro has been implemented to impose the periodic boundary conditions. The FE problem is formulated considering only the solid part of the domain, being the phononic crystal bandgap investigation referred to elastic waves in the structure and not to acoustic ones in the acoustic-structure interaction problem.[23] Such a conclusion has been corroborated by the execution of analyses that include the acoustic-structure interaction, finally obtaining that air modeling has no impact on the bandgap assessment. The Irreducible Brillouin Zone (IBZ),[1] that is the tetrahedron drawn in Fig. 1(b), corresponds to the simple cubic lattice structure.[6] Two bandgaps are highlighted: the first one endowed with a gap-mid gap ratio equal to 132.2%, and the

second one with 9.3%. The first one is the greatest gap-mid gap ratio in literature for three-dimensional phononic crystals, see Table I.

The unit cell analyzed in this work has a fundamental length $a = 0.05$ m, the geometry has the same proportions described above, and it is made of sintered Nylon PA2200[24] which, considering a pure linear elastic constitutive model, has Young's modulus $E_0 = 1750$ MPa, Poisson's coefficient $\nu = 0.4$ and density $\rho = 930$ kg/m$^3$. By considering the Nylon properties and the unit cell characteristic dimension, the first bandgap extends from 3.85 kHz to 18.87 kHz, while the second one from 21.95 kHz to 24.09 kHz. A finite structure composed of $4 \times 4 \times 3$ unit cells (see Fig. 3) has been produced through Selective Laser Sintering (SLS), an additive manufacturing process that has no need of support material (a critical issue for the realization of suspended parts, like spheres in this case) while guaranteeing good precision. The overall dimensions of the finite structure are 200 mm $\times$ 200 mm $\times$ 150 mm, for an air-solid volume ratio around 15% and a total weight of approximately 4.8 kg. The finite structure response is assessed both numerically, by means of a FE model, and experimentally.

The FE model of the finite structure has been developed in COMSOL Multiphysics v5.2, Solid Mechanics Module. Free boundary conditions are imposed to the structure in all the boundaries except from the central portion area of face A where a harmonic pressure that spans from 0.5 kHz to 20.0 kHz is applied. The output is measured on the central portion of face B and the transmission spectrum is determined. For the range of analyzed frequencies, the material behavior is better described by the visco-elastic model.[25,26] In this work, the damping is described by a Rayleigh model with coefficients $\alpha = 1$ s$^{-1}$ and $\beta = 4.0$e-7 s, and further a frequency dependence of Young's modulus is considered. Between 0.5 kHz and 20.0 kHz, Young's modulus $E(f)$ is assumed to increase with logarithmic trend from $E_0$ to $1.1E_0$ as experimentally assessed.[27]

The experimental setup is schematically represented in Fig. 4. Free boundary conditions are approximated using a soft material (i.e., bubble wrap) as base for the device. This configuration safely and uniformly sustains the crystal and does not sensibly affect its dynamics. The $4 \times 4$ side of the crystal leans against the base, so the bandgap is tested along a direction with 3 unit cells. The excitation is applied
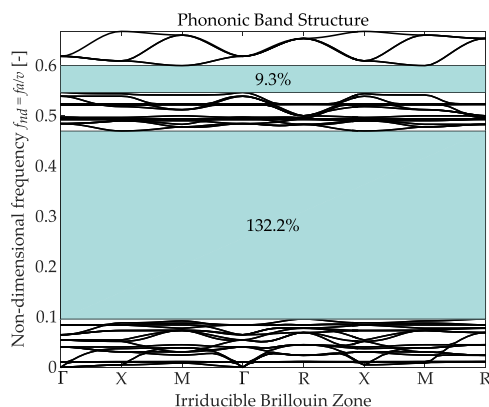


FIG. 2. Non-dimensional phononic band structure for the three-dimensional phononic crystal. The highlighted areas are the first two bandgaps. The number reported inside the bandgaps is the related gap-mid gap ratio in percentage. In the definition of the non-dimensional frequency $f_{nd}$, $f$ [Hz] is the frequency, $a$ [m] the unit cell dimension, and $v$ [m/s] the sound velocity in the medium.
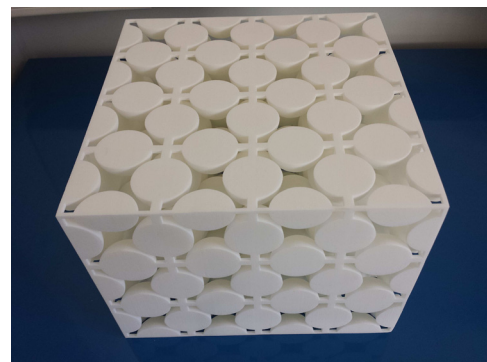


FIG. 3. Prototype of the finite crystal, composed by $4 \times 4 \times 3$ unit cells and made of Nylon PA2200 by additive manufacturing (SLS).
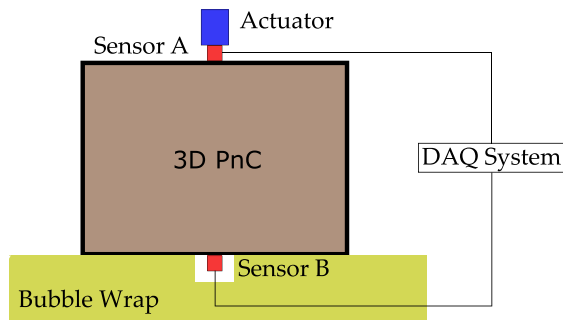
FIG. 4. Schematic representation of the experimental setup. One accelerometer is placed on top (A, below the actuator) and another one on the bottom (B) of the finite structure, connected to a data acquisition (DAQ) system. A bubble wrap is used to hold up the structure.

vertically using an inertial actuator, a VibeTribe-Troll with 10 W power and a frequency range from 40 Hz to 20 kHz. Two PCB Piezotronics 353B15 accelerometers, with a sensitivity of 10 mV/g and resonant frequency higher than 70 kHz, are placed at the center of faces (see Fig. 4): sensor A on top directly measures the input from actuator, while sensor B acquires the output signal. Acquisition chain is completed with a 8-channel ICP® Sensor Signal Conditioner, a PCB 483C05, and a NI 9205 module, with 16-bit resolution. Tests are performed with a slow sweep sine input from 0.5 kHz to 20.0 kHz, both sweep up and sweep down. Data are then post-processed in order to estimate the transmission spectrum.

The transmission diagram between the top face of the crystal and the bottom face is reported in Fig. 5 for both numerical and experimental results. The black dotted curve shows the numerically calculated transmission considering a linear elastic material with no dependency of its parameters from the excitation frequency. Although the considered crystal has finite dimensions, it can be seen that the bandgap initial and final frequencies (the vertical green dashed lines) are close to those of the infinite periodic crystal. Moreover, its resonance peaks around 14.0 kHz and 15.0 kHz are associated to resonances induced in the structure by the provided punctual excitation. The numerical prediction considering a



FIG. 6. Trend of the first and second bandgaps using different materials in the proposed geometry for the frame and the spheres. The material properties of the spheres are changed with respect to the ones of PA2200 by means of a multiplication factor for both Young's modulus $E$ and density $\rho$. Non-dimensional frequencies are obtained with the same scaling factors of Figure 2 referred to Nylon.

frequency-dependent Young's modulus and Rayleigh damping (red dashed curve) is in good agreement with the experimental measurements (blue solid curve). The attenuation is null till the initial bandgap frequency. It then reaches values of approximately 75 dB at the center of the bandgap, and it starts to decrease until the bandgap closing frequency. The effects of frequency dependent Young's modulus and damping can justify the larger width of the bandgap,[28] while a better non-linear visco-elastic model of Nylon PA2200 could improve the matching between numerical and experimental results in the high frequency range, i.e., from 18.0 kHz on. Furthermore, the larger bandgap width at high frequency can also be related to the $\Gamma - X$ path used as the preferential direction for the input forcing of the inertial shaker during the experimental tests.

In the present work, the authors show a 3D phononic crystal endowed with the widest full bandgap in literature.
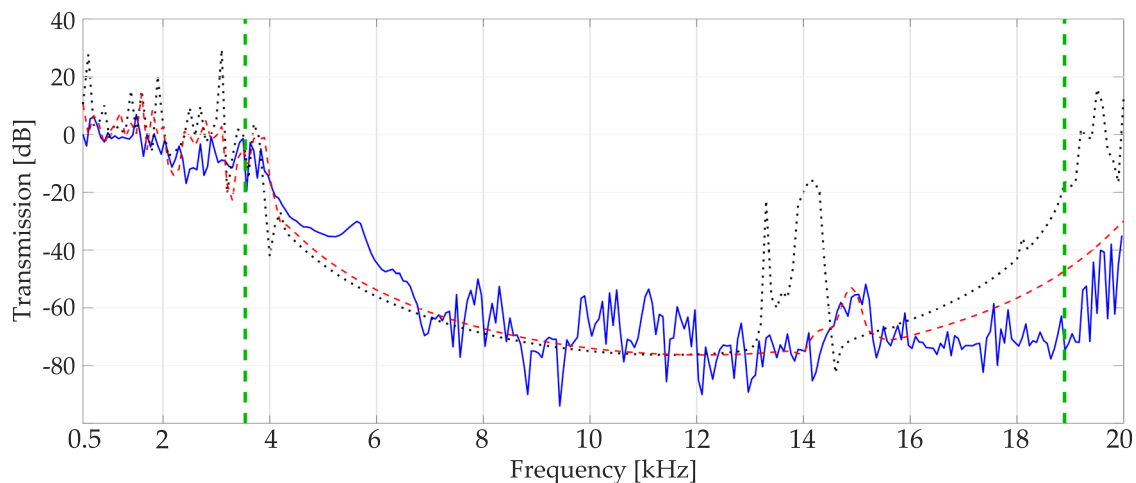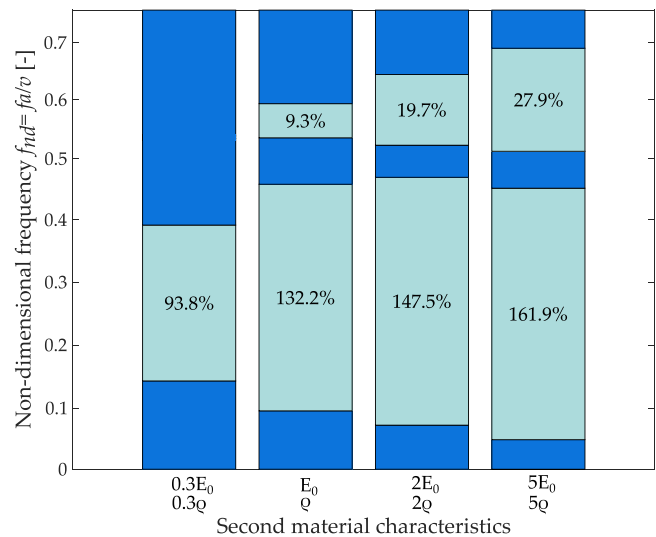


FIG. 5. Transmission diagram, in dB, between the central portion of the top face of the crystal and the opposite one: numerical linear elastic model with no material parameters dependency on the frequency (black dotted line), numerical with material parameters dependency on the frequency (red dashed line) and experimental (blue solid line). The two green vertical dashed lines represent the bottom and top limits of the first bandgap of the analyzed crystal.

An optimized topology of in-plane periodic crystal is extended to create a 3D crystal. An idea to further broaden the bandgap size, keeping the optimized geometry unaltered, is to introduce material inhomogeneity in order to enhance the difference of elastic impedances. Splitting the geometry into a beam frame and spheres of different material would modify the bandgap width as shown in Fig. 6. Multiplication factors of 0.3, 2, and 5 are considered for both Young's modulus and density with respect to PA2200 characteristics. It can be seen that, by using different materials, the gap-mid gap ratio can be increased up to 162%, while lowering the first bandgap starting frequency and strongly affecting the second bandgap. Of course, this is just a first attempt to consider the two materials inside the structure. A deeper analysis is however required to assess the technological feasibility.

To reduce the frequencies at which this bandgap occurs, resonant portions could be further introduced in the considered crystal in order to create a so-called elastic metastructure.[29]

[1] L. Brillouin, *Wave Propagation in Periodic Structures: Electric Filters and Crystal Lattices* (Dover Publications, Inc., New York, 1946).

[2] C. Kittel, *Introduction to Solid State Physics*, 8th ed. (Wiley, 2004).

[3] J. Joannopoulos, S. Johnson, J. Winn, and R. Meade, *Photonic Crystals: Molding the Flow of Light*, 2nd ed. (Princeton University Press, 2011).

[4] P. Deymier, *Acoustic Metamaterials and Phononic Crystals* (Springer-Verlag, Berlin, Heidelberg, 2013).

[5] M. Hussein, M. Leamy, and M. Ruzzene, "Dynamics of phononic materials and structures: Historical origins, recent progress, and future outlook," Appl. Mech. Rev. **66**, 040802 (2014).

[6] V. Laude, *Phononic Crystals: Artificial Crystals for Sonic, Acoustic, and Elastic Waves* (De Gruyter, 2015).

[7] M. Maldovan, "Sound and heat revolutions in phononics," Nature **503**, 209–217 (2013).

[8] V. Laude, "General solution of the coupled-wave equations of acousto-optics," J. Opt. Soc. Am. A **20**, 2307–2314 (2003).

[9] A. Khelif, B. Djafari-Rouhani, V. Laude, and M. Solal, "Coupling characteristics of localized phonons in photonic crystal fibers," J. Appl. Phys. **94**, 7944–7946 (2003).

[10] M. Maldovan and E. Thomas, "Simultaneous localization of phonons and photons in two-dimensional periodic structures," Appl. Phys. Lett. **88**, 251907 (2006).

[11] S. El-Jallal, M. Oudich, Y. Pennec, B. Djafari-Rouhani, V. Laude, J.-C. Beugnot, A. Martínez, J. Escalante, and A. Makhoute, "Analysis of opto-mechanical coupling in two-dimensional square lattice phoxonic crystal slab cavities," Phys. Rev. B **88**, 205410 (2013).

[12] O. Sigmund and J. Jensen, "Systematic design of phononic band-gap materials and structures by topology optimization," Philos. Trans. R. Soc., A **361**, 1001–1019 (2003).

[13] G. Gazonas, D. Weile, R. Wildman, and A. Mohan, "Genetic algorithm optimization of phononic bandgap structures," Int. J. Solids Struct. **43**, 5851–5866 (2006).

[14] O. Bilal and M. Hussein, "Ultrawide phononic band gap for combined in-plane and out-of-plane waves," Phys. Rev. E **84**, 065701(R) (2011).

[15] J.-H. Lee, C. Koh, J. Singer, S.-J. Jeon, M. Maldovan, O. Stein, and E. Thomas, "25th anniversary article: Ordered polymer structures for the engineering of photons and phonons," Adv. Mater. **26**, 532–569 (2014).

[16] X. Zhang, Z. Liu, Y. Liu, and F. Wu, "Elastic wave band gaps for three-dimensional phononic crystals with two structural units," Phys. Lett. A **313**, 455–460 (2003).

[17] T. Delpero, S. Schoenwald, A. Zemp, and A. Bergamini, "Structural engineering of three-dimensional phononic crystals," J. Sound Vib. **363**, 156–165 (2016).

[18] F. Lucklum and M. Vellekoop, "Realization of complex 3-D phononic crystals with wide complete acoustic band gaps," IEEE Trans. Ultrason. Ferroelectr. **63**, 796–797 (2016).

[19] S. Babaee, P. Wang, and K. Bertoldi, "Three-dimensional adaptive soft phononic crystals," J. Appl. Phys. **117**, 244903 (2015).

[20] T.-X. Ma, Y.-S. Wang, Y.-F. Wang, and X.-X. Su, "Three-dimensional dielectric phoxonic crystals with network topology," Opt. Express **21**, 2727–2732 (2013).

[21] L. D'Alessandro, B. Bahr, L. Daniel, D. Weinstein, and R. Ardito, "BESO approach to topology optimization of GaN phononic crystals," in VII European Congress on Computational Methods in Applied Sciences and Engineering (2016).

[22] It must be noted that the optimal topology strongly depends on the thickness of the slab and on the elastic parameters of the material adopted.

[23] S. Hedayatrasa, K. Abhary, M. Uddin, and C.-T. Ng, "Optimum design of phononic crystal perforated plate structures for widest bandgap of fundamental guided wave modes and maximized in-plane stiffness," J. Mech. Phys. Solids **89**, 31–58 (2016).

[24] EOS GmbH—Electro Optical Systems, "PA 2200—material data sheet."

[25] B. Merheb, P. Deymier, M. Jain, M. Aloshyna-Lesuffleur, S. Mohanty, A. Berker, and R. Greger, "Elastic and viscoelastic effects in rubber/air acoustic band gap structures: A theoretical and experimental study," J. Appl. Phys. **104**, 064913 (2008).

[26] B. Cotté, A. Parret-Fréaud, and A. Chaigne, "Measurement and modeling of damping for time-domain structural acoustics simulations," in Noise-Con 2013 (Denver, CO, USA, 2013).

[27] P. Collet, G. Gary, and B. Lundberg, "Noise-corrected estimation of complex modulus in accord with causality and thermodynamics: Application to an impact test," J. Appl. Mech. **80**, 011018 (2013).

[28] M. Hussein and M. Frazier, "Band structure of phononic crystals with general damping," J. Appl. Phys. **108**, 093506 (2010).

[29] K. Matlack, A. Bauhofer, S. Krödel, A. Palermo, and C. Daraio, "Composite 3D-printed metastructures for low-frequency and broadband vibration absorption," Proc. Natl. Acad. Sci. **113**, 8386–8390 (2016).